RESEARCH PAPER

Cobalt Thin Films Synthesis and Structural and Morphological Properties

A. Kharmouche

* *kharmouche_ahmed@univ-setif.dz & kharmouche_ahmed@yahoo.fr*

Laboratory of Surfaces and Interfaces Studies of Solid Materials (LESIMS), Department of Physics, Faculty of Technology, SETIF1 University Ferhat ABBAS, 19000, SETIF, Algeria

Received: January 2025 **Revised: February 2025** **Accepted: March 2025**
DOI: 10.22068/ijmse.3902

Abstract: *Series of cobalt (Co) thin films with various thicknesses ranging from 50 to 400 nm have been fabricated using thermal heating under a vacuum. We explore the impact of the thickness layer on the structural and morphological properties of the films. X-ray diffractions and atomic force microscopy tools have been used to carry out the structural and the morphological properties of these films. The films are principally c-axis oriented, polycrystalline and with <0001> texture. The crystallites' sizes have been found to range from 18.40 to 79.46 nm, and they increase with increasing thickness. The ratio c/a value indicates that Co films are subject to a tensile stress, probably because of the way the film grows. The microstrain is positive and ranges from 1.53% to 3.56%. Atomic force microscopy observations indicate the formation of crystallites according to the Stranski-Krastanov mode. The film's topographical surfaces are very smooth, the average root mean square roughness ranging from 0.2 to 1.5 nm.*

Keywords: *Co, Thin films, XRD, Crystallite size, AFM.*

1. INTRODUCTION

The rapid technological advancement in recent years in diverse branches of nanoscience has allowed the fabrication of new materials in the form of thin films with properties that do not exist in the bulk state. If the material is in a two-dimensional state, magnetic anisotropy is often generated. The comportment of the anisotropy is governed by several factors, specifically, the thickness of the magnetic layers and their microstructure, as well as the composition of the substrates or the surface roughness. The magnetic properties of these nanostructures find their application in the industrial field, mainly in the world of magnetic recording. These magnetic properties are strongly linked to the structural and morphological properties of the materials. Fundamental and applied research on cobalt and its binary and ternary alloys as thin films, as well as superlattices and dots, has been very prolific in recent decades [1-12].

Cobalt is a grim transition metal element. It is associated with methyl and constitutes a fragment of vitamin B-12. Cobalt is mainly utilized in electronic devices, specifically in magnetic recording media. Also, it is involved in catalysation for many chemical industries and in the production of rechargeable batteries, used in all phones and computers, as well as in electric vehicles. Cobalt is a chief constituent in numerous aerospace, security, and medical applications. It improves energy density in lithium-ion batteries and, therefore, contributes to lengthier driving ranges and stronger performance for electric vehicles. This brief summary of some performances of Cobalt encourages us to deepen the research concerning its physical properties and expand their applications. These physical properties depend significantly on the methods and conditions of production. Cobalt material has been investigated as thin films, dots, and part of multilayers. It has been prepared by means of several techniques, principally by sputtering [13], electrodeposition [14], thermal evaporation [15, 16], pulsed laser deposition [17)] and molecular beam epitaxy [18]. Since the late seventies of the twentieth century, when Prof. Iwasaki produced CoCr thin films characterized by perpendicular magnetic anisotropy, numerous investigations on the perpendicular recording media (PRM) have been undertaken.

To achieve a perpendicular magnetic anisotropy, it is indispensable to manufacture a media with an anisotropy energy that predominates over the demagnetizing energy. Obviously, this is closely related to the manufacturing conditions of thin films and their structural properties. Excellent morphological and structural as well as magnetic properties can be realised when depositing a single cobalt layer on monocrystalline Si substrates using the technique of thermal evaporation under

[DOI: 10.22068/ijmse.3902]

vacuum.
In this paper, we report experimental investigations on the physical properties of cobalt thin films synthesized by vacuum thermal evaporation, mainly the structural and morphological properties. Thickness measurements are accomplished by means of a Taylor-Hobson Talystep, and an x-ray diffraction (XRD) tool was employed to carry out the structural properties. To investigate the morphological and topographical images' surfaces and measure the roughness, we used an atomic force microscope (AFM).

2. EXPERIMENTAL PROCEDURES

2.1. Sample Preparation

We prepared a series of Co thin films via physical vapor deposition using a vacuum technique. The layers are deposited onto monocrystalline silicon substrate at room temperature, in a homemade working chamber (fig. 1). The main materials consist of 99.99% pure commercial powders, made and provided by Good Fellow GmbH Company. The substrates, whose surfaces are approximately equal to 1 cm^2, are fixed on a substrate holder located at a perpendicular distance of 7 cm above a tungsten boat covered with alumina (Al_2O_3) and containing a small quantity of the cobalt powder. Above this basket is placed a metallic plate. The role of this plate is to protect the samples when degassing the powders as well as to control and manage the deposit time; it is attached to a piston which can be manually operated from outside the bell. When the suitable pressure is reached, after hours of pumping, the evaporation process of the materials begins. The vacuum is ensured by two pumps, a primary pallet pump to reach a primary vacuum lesser than 10^{-3} mbar and a secondary oil diffusion pump to obtain a high vacuum of 10^{-7} mbar. This secondary pump is equipped with a cooling system. Once this 10^{-7} mbar base pressure is reached, we plug in the electrical current to initiate the evaporation. For this deposit, the suitable intensity of the electric current was maintained at 285 A, and the working pressure was less than 10^{-6} mbar. Lastly, the average deposition rate was maintained around 2 Å/s.

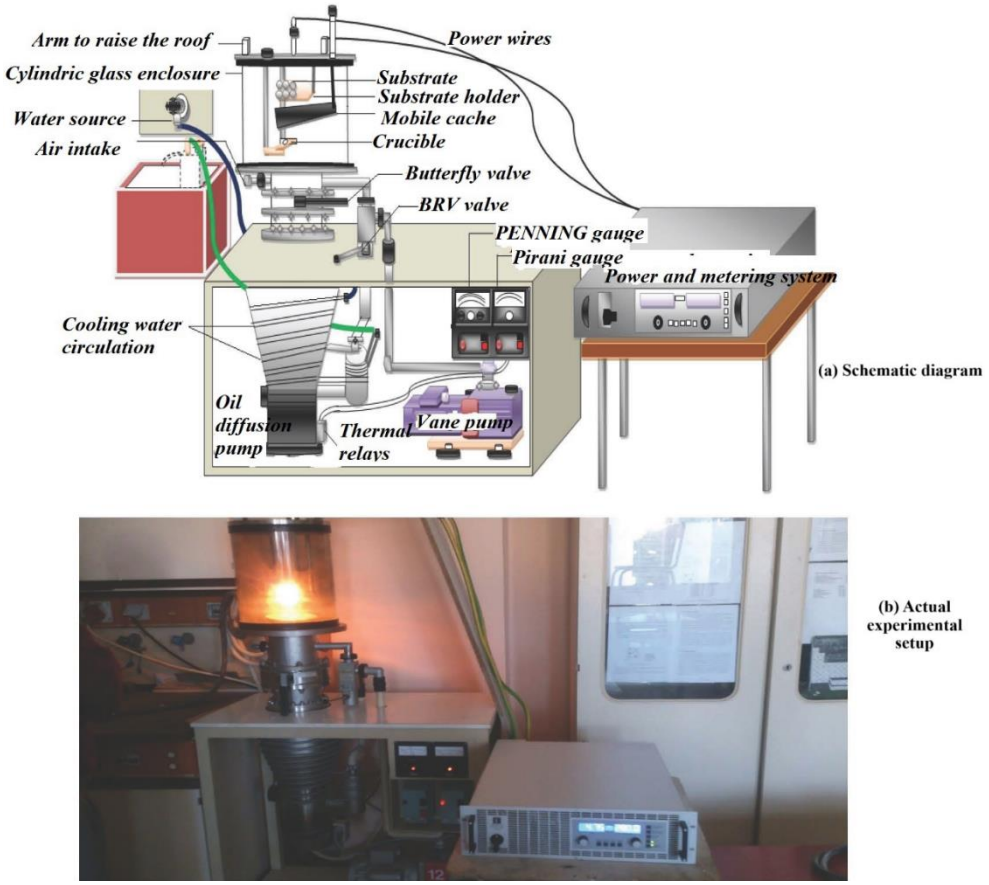

Fig. 1. Working evaporation chamber

[DOI: 10.22068/ijmse.3902]

2.2. Characterization Tools

The thickness of the evaporated Co films ranges from 50 to 400 nm, measured using a 'Taylor–Hobson' Talystep apparatus. With X-ray diffraction (XRD), we used a Siemens D-500 diffractometer, under a wavelength λ= 1.789 Å, in the "θ-2θ" scanning mode of the Bragg-Brentano geometry to probe the structural characterizations. The Diffractometer is working at 40 mA and 45 kV at a sweep angle 2θ ranging from 30° to 80°. We used Atomic Force Microscopy tools, using a Veeco 3100 apparatus in tapping mode, to investigate the morphology structure of our thin films and measure the surface roughness. More details on the characterization tools may be found in [19, 20].

3. RESULTS AND DISCUSSION

3.1. Structural Properties

3.1.1. Texture

We carried out the diffraction patterns of our Co thin films beneath the experimental conditions defined in Section 2. In order to study the influence of the thickness of the Co thin films on the evolution of the structural properties, examples of X-ray diffractograms, recorded for thin films of 50 and 200 nm, are presented in Fig. 2, in the 40-75° reduced array of the diffraction angle. These spectra infer that the prepared Co samples are polycrystalline. The films also present a hexagonal phase principally owing to the existence of the diffraction peaks with Bravais-Miller indices $(10\bar{1}0)$ and $(10\bar{1}1)$ with moderate intensity, and a high intensity peak (0002), correspondingly positioned at values of θ equal to 24.4°, 27.9° and 26.2° (i.e. 2θ equal to 48.8°, 55.8° and 52.4°). To evaluate the measured value of the texture, we consider the ratio among the diffraction peak intensity corresponding to the [0001] grains and the summation of the intensities of the (0001), $(10\,\bar{1}\,0)$ and $(10\,\bar{1}\,1)$ grains. Therefore, a value of 1 for the texture means that the growth is completely oriented along the [0001] axis:

$$< 0001 > \text{texture} = \frac{I_{0001}}{I_{0001}+I_{10\bar{1}\,1}+I_{10\bar{1}0}} \qquad (1)$$

This ratio is equal to 0.57 for the 50 nm Co thick film and to 0.72 for the 200 nm Co thick film (fig. 2). All the other values range from 0.6 to 0.85 as the film thickness increases from 100 to 400 nm. The films are then polycrystalline with <0001> texture. These planes, with the (0001) preferential orientation, are a little broad, and their intensity is higher when the thickness increases. This comportment is steady with the Van der Drift evolutionary model, which states that the texture is more marked as the film thickness increases [3, 21].

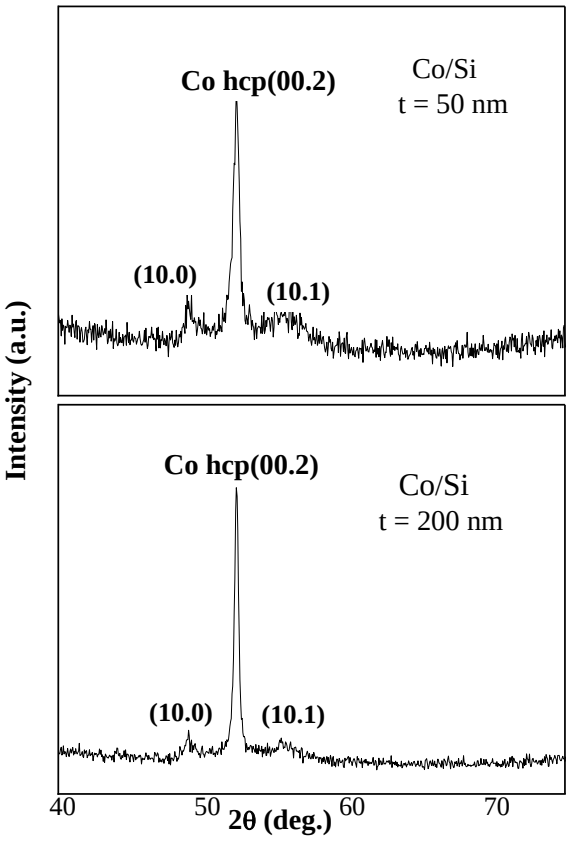

Fig. 2. Specimen of XRD spectra JCPDS Card#05-07

3.1.2. Crystallite size

Crystallite size ensures a significant effect on the physical properties of materials. The crystallite size is a parameter that allows for a measurable evaluation of the crystallinity of the films. The crystallite sizes can be defined as the mean value of the distance between the diffracting planes. The crystallite sizes deliver information about the thin films' conditions of production and their mechanical, electrical and magnetic properties [22]. With the aim of examining the crystallinity of our Co films, we investigated the growth of the crystallite size. Using the widely known Scherrer equation [23, 24], we have calculated the typical crystallite size D, exploiting the enlargement of the chief (0002) diffraction Bragg peak:

$$< D >= k\lambda/\Delta\cos\theta \qquad (2)$$

[DOI: 10.22068/ijmse.3902]

k being the Scherrer's constant, a dimensionless integer whose value is nearly 0.9; λ is the monochromatic wavelength of the radiation, its value in the current work being λ= 1.789 Å. Δ is the full width at half maximum (FWHM), corresponding to the greatest intense (0002) diffraction peak. We keep in mind that the full width at half maximum is inversely proportional to the crystallite size and is considered as a degree of the disorder in the material. θ is the Bragg diffraction angle situated at the topmost of this peak. Table 1 exhibits the average crystallite size of our Co thin films, and Fig. 3 shows the evolution of the crystallite size against the cobalt thickness. In this figure, the experimental points are the bold squares, and the continuous curve is just a guide for the eye. In Fig. 3, the D curve displays a monotonous increase with thickness, from 18.4 to 79.46 nm, as the Co thickness increases from 50 to 400 nm. Of course, large crystallite size is an autograph of good crystallinity and texture. Indeed, if a diffraction peak exhibits a low intensity and a broad enlargement, i.e., an important FWHM, the diffracted phase is then disordered, its crystallite size small and its crystalline quality poor. On the other hand, if a diffraction peak exhibits a high intensity and a finer enlargement, i.e., a small FWHM, the crystallite sizes are large, and this is characteristic of a well-crystallized phase. Films with large crystallite size are appropriate for application in magnetic sensors. This evolution of the crystallite size with thickness is predictable. Indeed, S.S. Soumya et al. produced post-annealed 600°C cobalt tin oxide thin films via the sol-gel spin coating procedure. They report that XRD analysis reveals that all the synthesized thin films were polycrystalline in nature and crystallize with tetragonal rutile structure with average crystallite size ranging from 4 to 11 nm [25]. Cherrad et al. synthesized Permalloy thin films onto monocrystalline silicone, using thermal heating under a vacuum. They measured crystallite size increasing from 8.6 to 19.6 nm as the thickness increases from 132 to 277 nm [26]. Using the conventional wet chemical co-precipitation method, M. P. Ghosh et al. produced several nanosized chromite samples with an overall arrangement of $Cu_xCo_{1-x}Cr_2O_4$. They confirmed that the x-ray diffraction profiles proved the existence of clean spinel crystal structure of the samples. By means of the Williamson-Hall method, they measured an average crystallite size of all the samples ranging from 11 to 16 nm [27]. Using the sol–gel method, Zhenyuan Li et al. synthesized ZnO nanoparticles and reported that X-ray diffraction measurements revealed that all films crystallized with a hexagonal wurtzite structure, and the crystallite size increased from 36 to 48 nm when the Bi content augmented from 0 to 7 mol% [28].

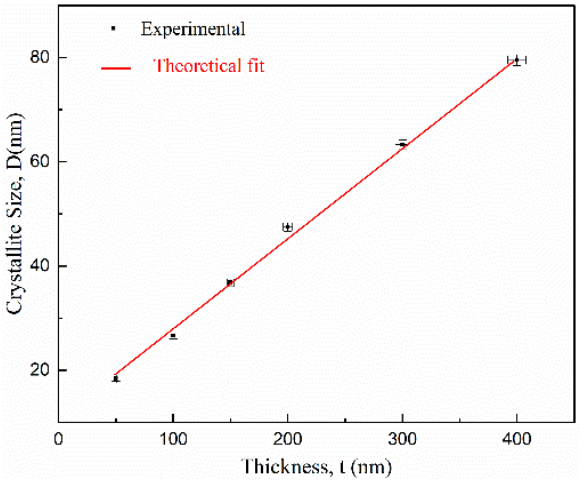

Fig. 3. Crystallite size as a function of Co thickness

3.1.3. Lattice parameters

X-ray diffraction also makes it possible to determine the mesh parameters from the Bragg equation and the quadratic form given by:

Bragg formula $2d_{hkl}\sin\theta = n\lambda$ (3)

The quadratic form $Q(hkl) = \frac{n^2}{[d(hkl)]^2} = \frac{4\sin^2\theta}{\lambda^2}$ (4)

h, k and l are the Miller indices of the crystalline planes, and d is the interplanar distance.

For the hcp structure (fig. 4), $a = b \neq c$ and $\alpha=\beta= 90°$ and $\gamma= 120°$, γ being the angle between a and b, α the angle between c and a, and β the angle between c and b, which leads to:

$$Q(hkl) = \frac{4}{3}\frac{h^2+k^2+hk}{a^2} + \frac{l^2}{c^2} \quad (5)$$

Therefore,

$$\frac{4\sin^2\theta}{\lambda^2} = \frac{4}{3}\frac{h^2+k^2+hk}{a^2} + \frac{l^2}{c^2} \quad (6)$$

In this case, there are two parameters to determine: a and c. These parameters are determined respectively by reflections of type (h k 0) and (0 0 l) because, by this type of reflections, there remains only one parameter to be determined.

Firstly, a value is determined when the Miller's indice l=0. This is possible for the (h k 0) diffracting planes. Then,

[DOI: 10.22068/ijmse.3902]

$$a = \frac{\lambda\sqrt{h^2+k^2+hk}}{\sqrt{3}\sin\theta} \quad (7)$$

Secondly, the c value is determined when the Miller's indices h=k= 0. This is possible for the (0 0 l) diffracting planes. Then,

$$c = \frac{\lambda l}{2\sin\theta} \quad (8)$$

In our case, we have this type of planes (002) and also (100) in the diffraction spectra of our Co thin films. The calculation of the values of a, c and c/a, determined for different thicknesses and crystallographic orientations, are presented in Table 1.

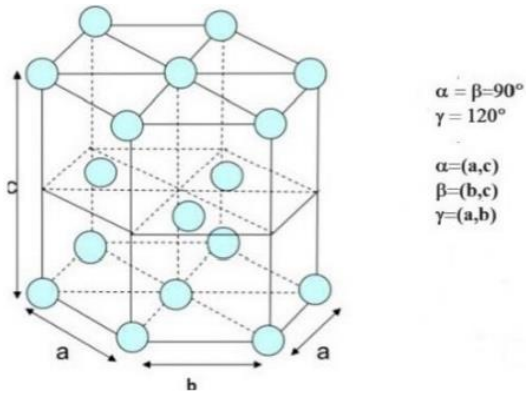

Fig. 4. Co hcp structure

Fig. 5 shows the variations of c/a as a function of Co layer thickness. The mean computed values range from 2.52 to 2.62 Å for a and from 4.17 to 4.42 Å for c; the ratio c/a increases from 1.655 to 1.688 as the Co thin film increases from 50 to 400 nm. Linked to the bulk parameters (a= 2.51 Å and c= 4.07Å, c/a= 1.63) [29, 30], our Co films are hence beneath a tensile stress, probably owed to the film's growth mode, a Stranski-Krastanov growing mode.

Fig. 6 shows the variations of c/a versus crystallite size, D. We observe that c/a increases monotonously with the increase of D. This increase of the lattice parameter has been reported by several authors. M. Mozaffari et al. observed that the lattice parameter of the samples increases with increasing Co content in their cobalt ferrite nanoparticles synthesized by the sol-gel method [31]. Abu-Elsaad et al. reported an increase of the lattice parameter with the addition of Co particles in their nano ferrites' thin films [32].

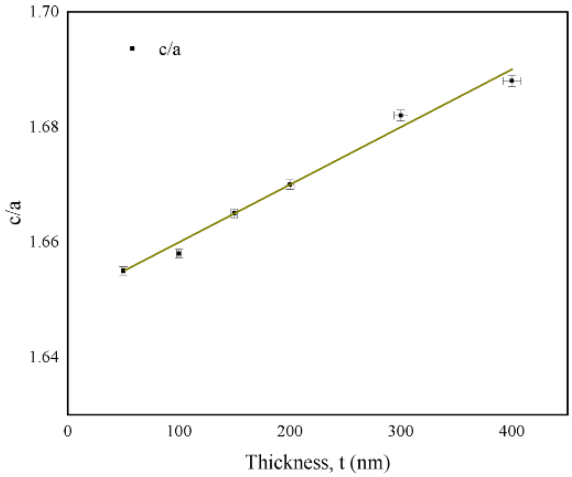

Fig. 5. Evolution of c/a as a function of Co thickness

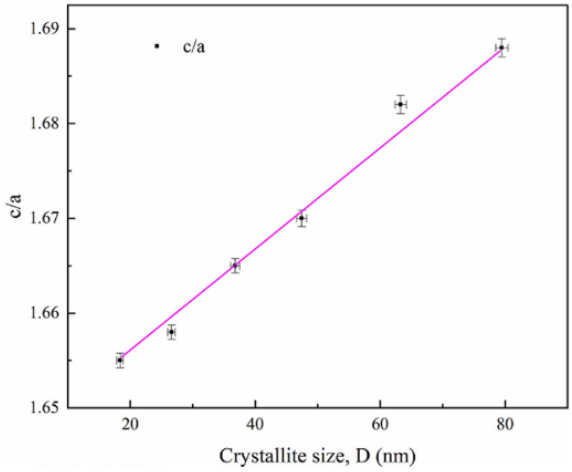

Fig. 6. Evolution of c/a as a function of crystallite size

3.1.4. Microstrain

We also computed the values of the microstrain ε (%), where

$$\varepsilon(\%) = \frac{c/a - c/a_{bulk}}{c/a_{bulk}} \quad (9)$$

Table 1. Crystallite size, D; lattice parameters a, c, and c/a ratio; microstrain, ε, and rms, w, as functions of Co layer thickness

t (nm)	50	100	150	200	300	400
D (nm)	18.40	26.62	36.82	47.46	63.28	79.46
a (Å)	2.52	2.54	2.57	2.58	2.60	2.62
c (Å)	4.17	4.21	4.28	4.31	4.37	4.42
c/a	1.655	1.658	1.665	1.670	1.682	1.688
ε (%)	1.53	1.72	2.15	2.45	3.19	3.56
w (nm)	0.20	0.35	0.60	0.80	1.10	1.50

[DOI: 10.22068/ijmse.3902]

These values are exhibited in Table 1 and the evolutions of the microstrain ε with respect to the thickness t, are depicted in Fig. 7. These values are positive and increase from 1.53 to 3.56%, as the film thickness increases from 50 to 400 nm, which infer that the films are under a low stress due probably to the mismatch lattice parameters between Co thin film and Si substrate. The fact that the microstrain values are positive indicates that the samples are under a tensile stress. This result confirms the conclusions found previously using the cell parameters values. In the literature, many researchers reported the existence of tensile microstrain. It is testified that numerous characteristics can lead to an increase ε, specifically lattice parameter mismatch and substitutions of atoms having a dissimilar atomic radius. Ghosh et al. reported tensile microstrains in all their samples of Cu ions substituted cobalt chromite nanoparticles prepared using conventional wet chemical co-precipitation method [27]. A. Goktas et al. measured positive values of the microstrain and a tensile strain in their nano rod-like homojunction thin films, prepared by chemical solution method [33]. Song et al. reported an increase of the microstress with an increase of the pressure in their pure cobalt thin films made-up by direct current magnetron sputtering [34].

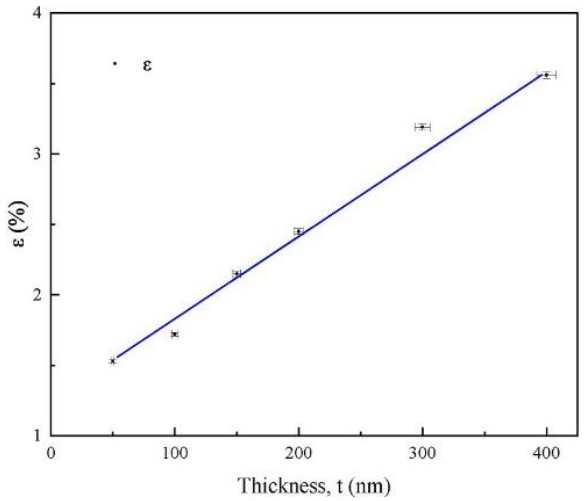

Fig. 7. Evolution of microstrain as a function of thickness

3.2. Morphological Properties

Because of their crucial role in the comprehension of particles comportment at the mesoscopic scale, particularly optical, electrical and magnetic behavior, the topographical and morphological properties of thin films surfaces need to be investigated with a considerable care. Surface morphology is tightly connected to the qualitative and quantitative features of the thin film surface, mainly the geometric form, the crystallites spreading and density, as well as the observation of probable defects. To this aim, we used atomic force microscopy (AFM), a non-destructive method, to explore the surface morphology and topography of our Co thin films.

The atomic force microscopy technique, developed in 1986 by Gerd Binnig, Calvin Quate and Christoph Gerber IBM researchers, is a type of very high-resolution local probe microscopy [35]. AFM analysis delivers images with near-atomic resolution to investigate surface topography.

This experimental procedure is capable of gauging the surface roughness of thin films down to the angstrom gauge. In addition to providing an image of the surface of the film, AFM analysis can also deliver quantifiable measurements of feature sizes, for example step heights and additional proportions. We achieved observations of the overall surface morphology and measure the average mean square roughness (rms) of our Co thin films. Examples of illustrative 2D and 3D AFM images are showed in Fig. 8.

These images show smooth, flat surfaces. All the samples present quasi-identical homogeneous surfaces devoid of craters and peaks, reflecting a good crystallinity. The 400 nm thickest film (c, f) displays an unchanging distribution of somewhat fine peaks on the total surface with a typical roughness of 1.5 nm. Table 1 exhibits the average rms roughness values, measured for all the Co thin films, and Fig. 9 displays the evolution of rms with the Co layer thickness. The rms values, w, increases with increasing thickness, from 0.2 to 1.5 nm. Other authors measured higher rms values for cobalt-based thin films. Tinouche et al. measured rms roughness up to 2.1 nm for Co thin films synthesized on GaAs substrate [36]. We observed topographic images with very rough surfaces full of craters and precipices in Co_xCr_{1-x}/Si(1 0 0) and Co_xCr_{1-x}/glass thin films [37]. Via electron beam evaporation procedure inside an UHV cavity, Anup Kumar Bera et al. reported rms roughness values ranging from 0.5 and 1.6 nm for their cobalt ultra-thin films grown on Si (100) [38].

[DOI: 10.22068/ijmse.3902]

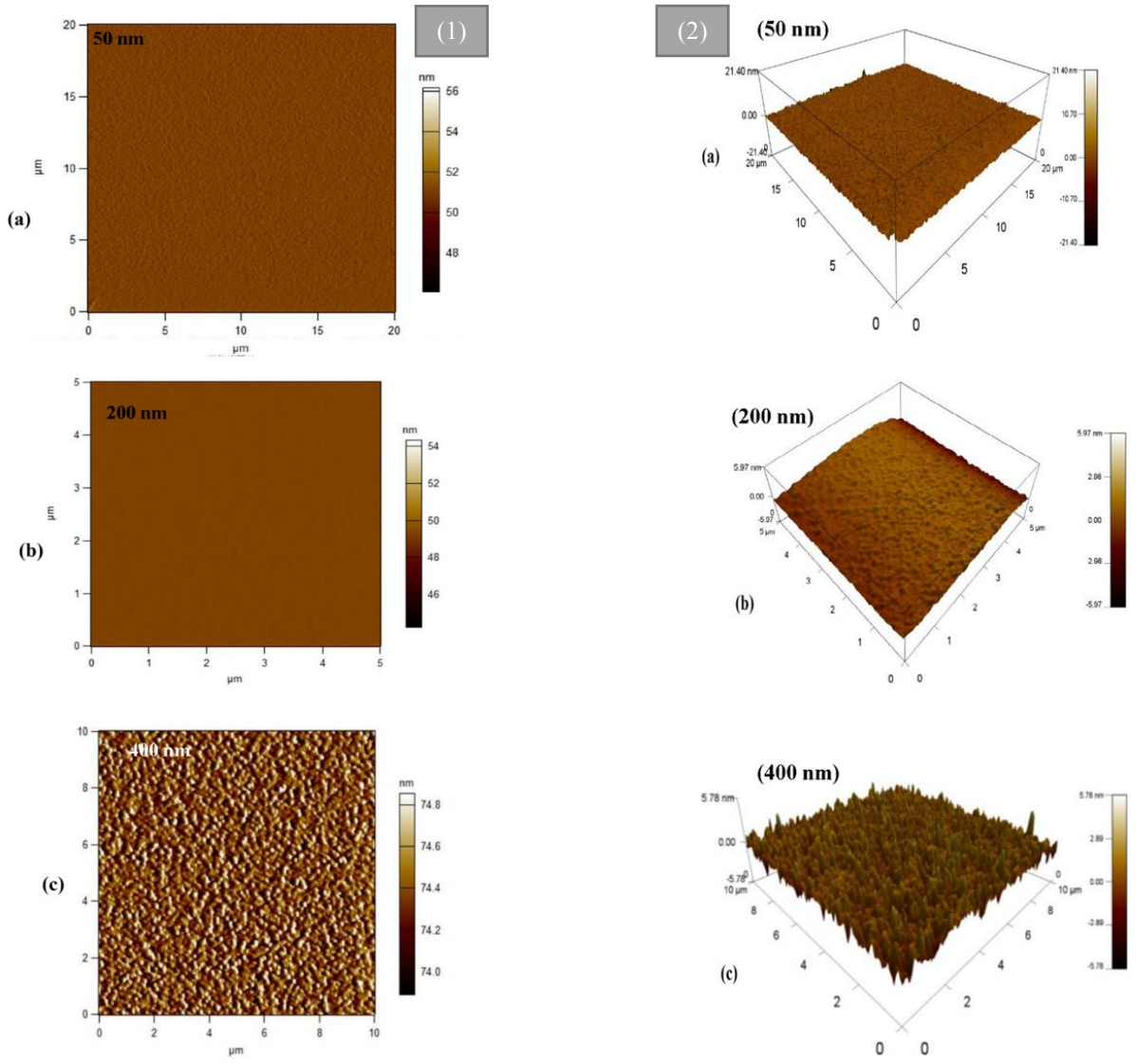

Fig. 8. (1) Specimen of 2D representative AFM images for a) 50 nm, b) 200 nm and c) 400 nm thin films. Scan area: 20 µm × 20 µm, 5 µm × 5 µm, 10 µm × 10 µm (2) Specimen of 3D representative AFM images for a) 50 nm, b) 200 nm and c) 400 nm thin films. Scan area: 20 µm × 20 µm, 5 µm × 5 µm, 10 µm × 10 µm

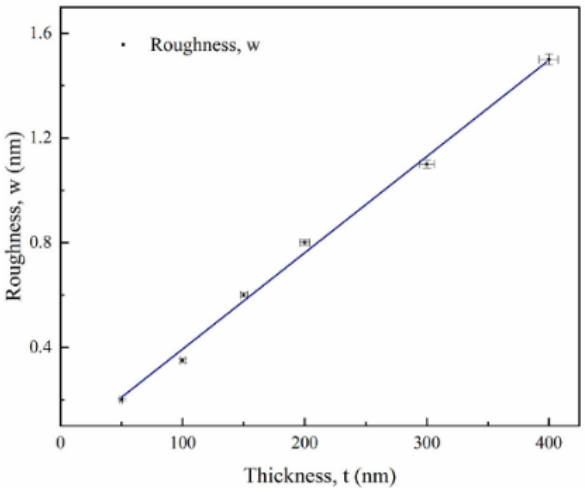

Fig. 9. Evolution of rms roughness with Co thickness

4. CONCLUSIONS

In this work, we prepared thin films of cobalt onto monocrystalline silicon, using thermal evaporation under a vacuum. We investigated the structural, topographical and morphological properties as functions of the thin film thickness. The thin films are polycrystalline with <0001> texture. The crystallites' sizes increase with increasing thickness and range in the mesoscopic scale, from 18.40 to 79.46 nm. The cell parameter values are higher than the bulk ones, and it is inferred that Co films are under tensile stress, probably due to the film's growth mode. This finding is corroborated by the positive values of the microstrain, ranging from 1.53% to 3.56%.

[DOI: 10.22068/ijmse.3902]

Atomic force microscopy observations indicate the formation of crystallites according to the Stranski-Krastanov mode. The film's topographical surfaces are very smooth, the average root mean square roughness ranging from 0.2 to 1.5 nm. These findings contribute to understanding the behavior of Cobalt based thin films at the mesoscopic scale.

ACKNOWLEDGMENTS

Thanks to the Algerian Directorate for Scientific Research and Technological Development (DGRSDT) for support.

CONFLITS OF INTEREST & STATEMENTS & DECLARATIONS

The author has followed compliance with ethical standards, which are the accepted principles of ethical and professional conduct.

RESEARCH DATA POLICY AND DATA AVAILABILITY STATEMENTS

The datasets generated and/or analysed during the current study are available from the corresponding author upon reasonable request.

CREDIT AUTHOR STATEMENT

Materials preparation was performed by A. Kharmouche. A. Kharmouche. A. Kharmouche carried out data collection and characterizations performed the first analyses. The final manuscript was written and approved by A. Kharmouche.

COMPETING INTERESTS

The authors have no relevant financial or non-financial interests to disclose.

REFERENCES

[1]. S. Iwasaki, ‘‘Perpendicular magnetic recording’’. IEEE Trans. Magn. MAG, 1980, 16, 71-76. https://doi.org/10.1109/TMAG.1980.1060546.

[2]. F. Nguyen-Van-Dau, M. Sussiau, A. Schuhl, P. Galtier, ‘‘Magnetic thin films having a lateral nano structural periodicity’’. J. Appl. Phys., 1997, 81, 4482–4484. https://doi.org/10.1063/1.364985.

[3]. S.M. Cherif, Y. Roussigné, A. Kharmouche, T. Chauveau, and D. Billet, ‘‘Effect of grain misorientation on the stripe domains in evaporated cobalt films’’, Eur. Phys. J. B, 2005, 45, 305–309. https://doi.org/10.1140/epjb/e2005-00190-7.

[4]. A. Kharmouche, Y. Roussigné, S.-M. Chérif, G. Schmerber, ‘‘Effect of Cr on the magnetic properties of evaporated Co_xCr_{1-x}/Si(1 0 0) and Co_xCr_{1-x}/glass thin films’’. Appl. Surf. Sci., 2009, 255, 6173–6178. http://dx.doi.org/10.1016/j.apsusc.2009.01.082.

[5]. A. Kharmouche, ‘‘Magnetic anisotropy factors of vapor deposited CoCr thin films on Si and glass substrates’’. J. Magn. Magn. Mater., 2013, 327, 91–94. https://dx.doi.org/10.1016/j.jmmm.2012.09.015.

[6]. N. Guechi, A. Bourzami, A. Guittoum, A. Kharmouche, S. Colis, N. Meni, ‘‘Structural, magnetic and electrical properties of Fe_xNi_{100-x}/Si(100) films’’. Physica B, 2014, 441, 47-53. http://dx.doi.org/10.1016/j.physb.2014.01.023.

[7]. M. Tinouche, A. Kharmouche, G. Schmerber, ‘‘Structural and Magnetic Studies of CoCr Thin Films Prepared by Physical Vapor Deposition’’. J Supercond Nov Magn, 2013, 26, 769–772. https://doi.org/10.1007/s10948-012-1914-5.

[8]. A. Bourezg, A. Kharmouche, ‘‘Synthesis, structural and magnetic properties of $Co_{100-x}Pd_x$/GaAs thin films’’. Vacuum, 2018, 155, 612–618. https://doi.org/10.1016/j.vacuum.2018.06.062.

[9]. A. Melloul, A. Kharmouche, ‘‘Synthesis, structure and magnetic properties of Co_xFe_{100-x} thin films thermally evaporated onto Si (111) substrate’’. J Mater Sci: Mater Electron, 2019, 30, 13144–13150. https://doi.org/10.1007/s10854-019-01677-3.

[10]. A. Kharmouche, ‘‘Magnetic Studies of Vapor-Deposited Co/Si(100) and Co/Glass Thin Films’’. J Supercond Nov Magn, 2011, 24, 591-595. https://doi.org/10.1007/s10948-010-0952-0.

[11]. N. Guechi and A. Kharmouche, ‘‘Structural, microstructural, electrical, and magnetic properties of $(Fe_xNi_y)_{100-z}Co_z$ ternary films’’. J Mater Sci: Mater Electron, 2023, 34, 2119. https://doi.org/10.1007/s10854-023-11544-x.

[DOI: 10.22068/ijmse.3902]

[12]. A. Kharmouche, ‘‘Anisotropy Factors of Co-Based Thin Films Computed from FMR and AGFM Studies’’. J Supercond Nov Magn, 2017, 30, 3295–3299. https://doi.org/10.1007/s10948-016-3803-9.

[13]. Mahdi Jamali, Yang Lv, Zhengyang Zhao, and Jian-Ping Wang, ‘‘Sputtering of cobalt film with perpendicular magnetic anisotropy on disorder-free graphene’’. AIP ADVANCES, 2014, 4, 107102, 5p. https://doi.org/10.1063/1.4897333.

[14]. Kwiyong Kim, Darien Raymond, Riccardo Candeago & Xiao Su. ‘Selective cobalt and nickel electrodeposition for lithium-ion battery recycling through integrated electrolyte and interface control’. Nat Commun, 2021, 12, 6554, 10p. https://doi.org/10.1038/s41467-021-26814-7.

[15]. Sushil, Sri Aurobindo Panda, Subhashis Gangopadhyay, Growth and characterization of Cobalt Oxide thin films. ICONNSLE2022: International Conference on Nanotechnology for Sustainable Living and Environment, Pilani, India, April 14-16, 2022. Materials Today: Proceedings, Volume 76, Part 2, 2023, Pages 449-452. https://doi.org/10.1016/j.matpr.2022.12.193.

[16]. A. Kharmouche, ‘‘an experimental study of the static magnetic properties of Co thin films’’. Eur. Phys. J. B, 2024, 97, 87, 9p. https://doi.org/10.1140/epjb/s10051-024-00729-w.

[17]. M.H. Ehsani, M. Jalali Mehrabad, P. Kameli, ‘‘Fabrication of Co thin films using pulsed laser deposition method with or without employing external magnetic field’’. J. Magn. Magn. Mater., 2016, 417, 117–121. https://doi.org/10.1016/j.jmmm.2016.05.074.

[18]. W. Dobrogowski, R. Gieniusz, U. Guzowska, Z. Kurant, I. Sveklo, A. Wawro, A. Maziewski, ‘‘Magnetic properties of Pt/Co/Pt trilayers with W insert layer’’. J. Magn. Magn. Mater., 2023, 587, 171339. https://doi.org/10.1016/j.jmmm.2023.171339.

[19]. Kharmouche, O. Cherrad, ‘‘Structural, microstructural and morphological properties of Permalloy/Si (100) thin films’’. Physica B: Condensed Matter, 2024, 680, 415803, 10p. https://doi.org/10.1016/j.physb.2024.415803.

[20]. A. Kharmouche and O. Cherrad, ‘‘Electrical properties of permalloy/Si (100) thin films’’. J Mater Sci: Mater Electron, 2024, 35, 759, 12p. https://doi.org/10.1007/s10854-024-12482-y.

[21]. A. Van der Drift, ‘‘Evolutionary selection, a principle governing growth orientation in vapour-deposited layer’’., Philips Res. Repts, 1967, 22, 267–288. https://projects.iq.harvard.edu/files/taolab/files/evolutionary_selection_ref.pdf.

[22]. Eberhart, J.-P. Structural and Chemical Analysis of Materials: X-ray, Electron and Neutron Diffraction; X-ray, Electron and Ion Spectrometry; Translated by J.P. Eberhart. Chichester, West Sussex, England, New York: Wiley, 1991.

[23]. A. Benhamoud, A. Kharmouche, ‘‘Synthesis, Structural, and Magnetic Properties of $Fe_{100-x}Pd_x$ Thin Films’’. J Supercond Nov Magn, 2020, 33, 1521–1526. https://doi.org/10.1007/s10948-019-05412-1.

[24]. A. Kharmouche and A. Melloul, ‘‘Structural and Magnetic Studies of Co_xFe_{100-x} Thin Films Thermally Evaporated on Glass’’. J Mater Sci: Mater Electron, 2020, 31, 19680–19690. https://doi.org/10.1007/s10854-020-04494-1.

[25]. S.S. Soumya, T.S. Xavier, ‘‘Effect of cobalt doping on the microstructural, optical and electrical properties of SnO_2 thin films by sol-gel spin coating technique’’. Physica B, 2022, 624, 413432. https://doi.org/10.1016/j.physb.2021.413432.

[26]. O. Cherrad and A. Kharmouche, ‘‘Thickness dependent physical properties of evaporated permalloy/GaAs(100) thin films’’. Eur. Phys. J. Appl. Phys., 2023, 98, 14, 13 p. https://doi.org/10.1051/epjap/2023220262.

[27]. Mritunjoy Prasad Ghosh, Sipun Mohanty, Riya Roy, Souvik Chatterjee, Samrat Mukherjee, ‘‘Investigations of the structure and tunable magnetic properties of Cu doped cobalt chromite nanoparticles’’. Jour. Magn. Magn. Mat., 2024, 590, 171632. https://doi.org/10.1016/j.jmmm.2023.171632.

[28]. Zhenyuan Li, Hui Li, Yong Chen & Maohua Wang, ‘‘Role of Bismuth Doping on Structural and Electrical Properties of ZnO Nanocrystals Prepared by Sol–Gel

[DOI: 10.22068/ijmse.3902]

Method''. J. Electron. Mater., 2024, 53, 2504–2513. https://doi.org/10.1007/s11664-024-10972-7.
[29]. Hofer, Peebles, J. Am. Chem. Soc., 68, 897(1947). JCPDS Card#05-0727.
[30]. A. Kharmouche, S-M. Chérif, A. Bourzami, A. Layadi and G. Schmerber, ''Structural and magnetic properties of evaporated Co/Si(100) and Co/glass thin Films''. J. Phys. D: Appl. Phys., 2004, 37, 2583–2587. http://dx.doi.org/10.1088/0022-3727/37/18/014.
[31]. M. Mozaffari, J. Amighian, E. Darsheshdar, ''Magnetic and structural studies of nickel-substituted cobalt ferrite nanoparticles, synthesized by the sol-gel method''. Jour. Magn. Mat., 2014, 350, 19–22. http://dx.doi.org/10.1016/j.jmmm.2013.08.008.
[32]. N.I. Abu-Elsaad, A.S. Nawara, S.A. Mazen, ''Synthesis, structural characterization, and magnetic properties of Ni-Zn nanoferrites substituted with different metal ions (Mn^{2+}, Co^{2+}, and Cu^{2+})''. J. Phys. Chem. Solids, 2020, 146,109620. https://doi.org/10.1016/j.jpcs.2020.109620.
[33]. Abdullah Goktas, Sait Modanlı, Ahmet Tumbul, Ahmet Kilic, ''Facile synthesis and characterization of ZnO, ZnO:Co, and ZnO/ZnO:Co nano rod-like homojunction thin films: Role of crystallite/grain size and microstrain in photocatalytic performance''. J. Alloys Compd., 2022, 893, 162334. https://doi.org/10.1016/j.jallcom.2021.162334
[34]. Kerui Song, Zhou Li, Mei Fang, Zhu Xiao and Qian Lei, ''Structural and magnetic properties of micropolycrystalline cobalt thin films fabricated by direct current magnetron sputtering''. Int J Miner Metall Mater, 2024, 31, 384–394. https://doi.org/10.1007/s12613-023-2715-5.
[35]. G. Binnig, C. F. Quate, and Ch. Gerber. ''Atomic Force Microscope''. Phys. Rev. Lett., 1986, 56, 930-933. https://doi.org/10.1103/PhysRevLett.56.930.
[36]. M. Tinouche, A. Kharmouche, B. Aktaş, F. Yildiz, A. N. Koçbay, ''Magnetic and Structural Properties of Co Thin Films Evaporated on GaAs Substrate''. J Supercond Nov Magn, 2015, 28, 921–925. https://doi.org/10.1007/s10948-014-2863-y.
[37]. A. Kharmouche, S.-M. Chérif, G. Schmerber, A. Bourzami, Magnetic and structural properties of evaporated Co_xCr_{1-x}/Si(1 0 0) and Co_xCr_{1-x}/glass thin films, Jour. Magn. Magn. Mat., 2007, 310, 152–158. https://doi.org/10.1016/j.jmmm.2006.08.012.
[38]. Anup Kumar Bera, Pooja Gupta, Debi Garai, Ajay Gupta, Dileep Kumar, ''Effect of surface morphology on magnetization dynamics of cobalt ultrathin films: An in-situ investigation''. Appl. Surf. Sci. Adv., 2021, 6, 100124. https://doi.org/10.1016/j.apsadv.2021.100124.

[DOI: 10.22068/ijmse.3902]